Magnetic Structures in the MnSb-CrSb System

W. J. TAKEI, D. E. COX, AND G. SHIRANE*
Westinghouse Research Laboratories, Pittsburgh, Pennsylvania
(Received 16 August 1962)

A magnetic and neutron diffraction investigation has been made on MnSb, CrSb, and their solid solutions, which crystallize in the hexagonal NiAs-type structure. MnSb is ferromagnetic and CrSb antiferromagnetic. As CrSb is substituted into MnSb, a canted spin structure is formed, the spins lying within ferromagnetic (001) sheets with the spins in adjacent sheets alternating in direction. The angle of cant increases with increasing Cr content in agreement with the model of de Gennes who considered the effects of double exchange on an antiferromagnetic system. The magnetic structure of CrSb consists of ferromagnetic (001) planes which are coupled antiferromagnetically. The spin axis is parallel to c. Between this structure and the canted spin structure with the spins perpendicular to c is an intermediate region. This antiferromagnetic region has either a tilted spin axis structure or two coexisting structures.

MnSb was found to have a change in the spin direction from a perpendicular to a parallel orientation with respect to c as the temperature was increased. The temperature of the spin flip was found to depend on the preparative conditions as did the Curie temperature and saturation moment.

I. INTRODUCTION

THE nickel arsenide structure is often found in compounds of the transition metals with metalloids.[1] This hexagonal structure, shown in Fig. 1, has the metal atoms arranged in a simple hexagonal lattice while the metalloids, considered alone, form a hexagonal close-packed arrangement. Magnetic ordering is found in many of these compounds.[2,3] Of particular interest for the study of the magnetic interactions are investigations of solid solutions between a ferromagnetic and an antiferromagnetic NiAs-type compound. One such system which has been studied previously is the solid solution between ferromagnetic MnSb and antiferromagnetic CrSb. A neutron diffraction investigation by Snow[4] reported that CrSb had ferromagnetic (001) planes with alternate planes coupled antiferromagnetically, and a spin axis parallel to c. Pickart and Nathans[5] reported MnSb to have the same spin direction. The results of magnetic measurements by Hirone *et al.*[6] and by Lotgering and Gorter[7] are essentially in agreement with each other and the transition temperatures found by the former authors are shown in Fig. 2(a). Solutions with large Mn contents show a Curie temperature and their saturation moments decrease rapidly with increasing Cr content. Compounds with large Cr contents show an anomaly in the susceptibility which was attributed to an antiferromagnetic transition. Solutions near 75% Cr seem to show both a Curie and a Néel temperature.

Several models were proposed for the magnetic structures in this system. Lotgering and Gorter[7] suggested

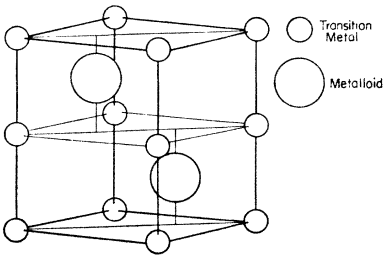

FIG. 1. Hexagonal unit cell of NiAs structure.

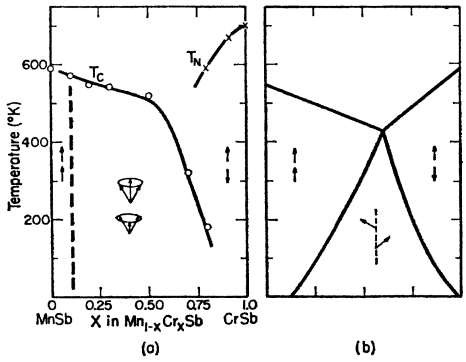

FIG. 2. Phase diagrams for $Mn_{1-x}Cr_xSb$ solid solutions. (a) Hirone *et al.* (reference 6); (b) de Gennes (reference 10).

that the Mn and Cr ordered independently, the Mn forming a ferromagnetic system and the Cr an antiferromagnetic one. Hirone and Adachi[8] made an analysis of NiAs compounds using the molecular field approximation and including three different interactions. They concluded that, according to the relative values of the interactions, various magnetic structures would be stable. They proposed that in the MnSb-CrSb solid solutions, a "triangular" spin structure with multispin

* Present address: Brookhaven National Laboratory, Upton, New York.

[1] A. J. Cornish, Acta Met. **6**, 371 (1958).
[2] K. Adachi, J. Phys. Soc. Japan **16**, 2187 (1961).
[3] T. Hirone, *Landolt Börnstein* (Springer-Verlag, Berlin, 1962), Anfage 6, Band II.
[4] A. I. Snow, Phys. Rev. **85**, 365 (1952).
[5] S. J. Pickart and R. Nathans, Suppl. J. Appl. Phys. **30**, 280S (1959).
[6] T. Hirone, S. Maeda, I. Tsubokawa, and N. Tsuya, J. Phys. Soc. Japan **11**, 1083 (1956).
[7] F. K. Lotgering and E. W. Gorter, J. Phys. Chem. Solids **3**, 238 (1957).
[8] T. Hirone and K. Adachi, J. Phys. Soc. Japan **12**, 156 (1957).

axes was present. A neutron diffraction study of antiferromagnetic CrSe by Corliss *et al.*[9] revealed a spin arrangement very similar to this type of structure.

De Gennes[10] made a theoretical analysis of the effects of double exchange on an antiferromagnetic system. Double exchange is a ferromagnetic interaction which was postulated by Zener[11] as arising from the presence of mobile carriers (electrons or holes). As the carriers "hop" from one atom to another, the energy is minimized when the atomic spins are parallel, i.e., there is ferromagnetic ordering. Anderson and Hasegawa[12] showed that the energy varied as $\cos(\Theta/2)$, where Θ is the angle between the atomic spins. De Gennes concluded that since the antiferromagnetic exchange energy varied as $\cos\Theta$, the ground-state energy is lowered when the two antiferromagnetic sublattices are canted with respect to each other. This would result in a ferromagnetic component. He proposed a generalized magnetic phase diagram for such a system as shown in Fig. 2(b) and suggested that it would apply to the $Mn_{1-x}Cr_xSb$ system if electron transfer is allowed between the Mn and Cr atoms. For most compositions, two transition temperatures were proposed, a high-temperature Curie or Néel point and, at lower temperatures, a transition to a canted structure. This theory has been applied to the magnetic properties of the[10] $La_{1-x}Ca_xMnO_3$ and[13] $Li_xMn_{1-x}Se$ systems. One difference of this canted model compared to the triangular model of Hirone and Adachi is in the periodicity of the spin structure. De Gennes' model has parallel spins within each (001) plane, the cant occurring between planes. Therefore, the magnetic unit cell is the same size as the chemical cell. Hirone and Adachi's model has three spin directions within each (001) plane and, thus, requires a larger unit cell.

Pickart and Nathans[5] made a neutron diffraction investigation of one composition in the series, $Mn_{0.2}Cr_{0.8}Sb$, which was reported to have Néel and Curie temperatures of 600 and 130°K, respectively. At room temperature, they found, as expected, an antiferromagnetic structure like that found in CrSb. However, at 4.2°K several weak superlattice reflections were present which could be indexed by tripling a and b. These were in addition to the magnetic contributions from a CrSb-type structure which had a moment decreased in magnitude compared with that at room temperature. Their conclusion was that neither the model of Lotgering and Gorter nor that of Hirone and Adachi was in agreement with their results. The model of de Gennes, which was published subsequent to Pickart and Nathans' investigation, would not explain these results either. In an attempt to clarify our understanding of this system, it was decided to make a more extensive investigation.

TABLE I. Lattice parameters for $Mn_{1-x}Cr_xSb$.

	a (Å)	c (Å)	c/a
MnSb (annealed)	4.130	5.789	1.402
MnSb (quenched)	4.15_3	5.77_1	1.390
$Mn_{0.75}Cr_{0.25}Sb$	4.106	5.778	1.407
$Mn_{0.49}Cr_{0.51}Sb$	4.097	5.697	1.391
$Mn_{0.30}Cr_{0.70}Sb$	4.104	5.625	1.371
$Mn_{0.25}Cr_{0.75}Sb$	4.107	5.598	1.363
$Mn_{0.20}Cr_{0.80}Sb$	4.108	5.584	1.359
$Mn_{0.15}Cr_{0.85}Sb$	4.111	5.560	1.352
CrSb	4.121	5.467	1.327

II. EXPERIMENTAL PROCEDURE

A. Sample Preparation and X-Ray Examination

The starting materials were 99.9% Cr from Electrometallurgical Associates, 99+% Mn from Belmont Smelting and Refining Company, and 99.999% Sb from American Smelting and Refining Company. After grinding, stoichiometric amounts of the elements were pressed and sealed in evacuated quartz tubes. The samples were heated slowly to 650°C, held at this temperature for 1 hr, then annealed at a temperature between 650 and 900°C for 24 h. The annealing temperatures were chosen so that the samples did not melt. The samples were reground and the annealing repeated. They were then cooled at the rate of 50°C/h except for the annealed MnSb and $Mn_{0.25}Cr_{0.75}Sb$ which were cooled at 15°C/h. Another sample of MnSb was prepared for us by A. Cornish of these Laboratories. This sample was removed from the furnace while at the preparative temperature and allowed to air cool. For convenience, this sample will hereafter be called "quenched" MnSb.

X-ray powder patterns were taken with CuK_α radiation using a thin Al foil to reduce the fluorescent radiation. All the patterns were extremely sharp for the samples reported in Table I except for the quenched MnSb. When MnSb and $Mn_{0.75}Cr_{0.25}Sb$ were prepared by cooling at 50°/h, they were found to give broad lines for 2θ greater than 120°. No trace of free metal or Sb was detectable in any of the samples.

The lattice parameters are shown in Fig. 3 and listed in Table I. For comparison, the results of Lotgering and Gorter,[7] who reported a possible error of "several hundredths of an angstrom," are also included. The present results are in agreement with the previous ones. Since they are determined with higher accuracy, the trends are now more clearly established. It should be noted that the scales in the figure for a and c are different so that the total variation of c is an order of magnitude larger than that of a. A difference of the same order in

[9] L. M. Corliss, N. Elliot, J. M. Hastings, and R. L. Sass, Phys. Rev. **122**, 1402 (1961).
[10] P.-G. de Gennes, Phys. Rev. **118**, 141 (1960).
[11] C. Zener, Phys. Rev. **82**, 403 (1951).
[12] P. W. Anderson and H. Hasegawa, Phys. Rev. **100**, 675 (1955).
[13] R. R. Heikes, T. R. McGuire, and R. J. Happel, Jr., Phys. Rev. **121**, 703 (1961).

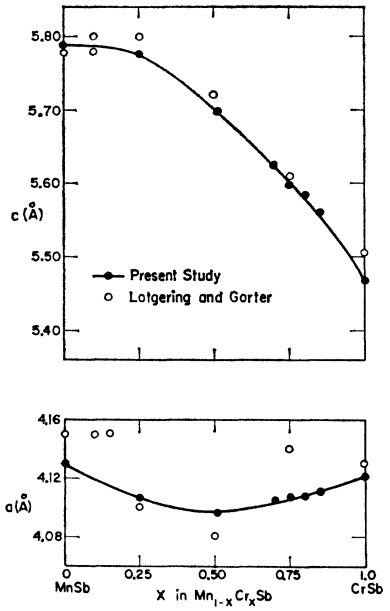

FIG. 3. Lattice parameters of $Mn_{1-x}Cr_xSb$ solid solutions. Solid circles are results of the present study and open circles, those of Lotgering and Gorter (reference 7).

the variation of c and a with temperature was found for pure MnSb by Willis and Rooksby.[14] The variation of the c/a ratio for the solid solutions is shown in Fig. 4. There is an initial increase in the ratio as Cr is added followed by a rapid decrease to the value for CrSb.

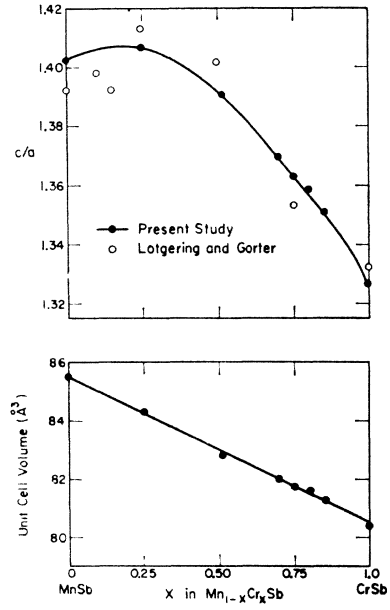

FIG. 4. Volume and c/a ratio of $Mn_{1-x}Cr_xSb$ solid solutions. Solid circles are results of the present study and open circles, those of Lotgering and Gorter, (reference 7).

[14] B. T. M. Willis and H. P. Rooksby, Proc. Phys. Soc. (London) Ser B **67**, 290 (1954).

Despite these variations in the dimensions of the unit cells, Fig. 4 shows that the volume is a linear function of the composition.

B. Magnetic and Neutron Diffraction Techniques

The magnetic measurements were made on a balance[15] based on the Faraday method. Measurements were made in fields up to 10 000 Oe and at temperatures from 77 to approximately 900°K. The Néel temperatures were taken as the inflection points of the susceptibility curves. As far as possible, the Curie temperatures were determined by the method of Weiss and Forrer[16] utilizing plots of field versus temperature at constant moment. The moments were extrapolated to infinite field from moment versus $1/H$ curves.

The neutron diffraction experiments were conducted at the Westinghouse Testing Reactor using a beam of 1.14 Å wavelength. The samples, which were all powders, were placed in 3/8-in. diameter, thin-walled, aluminum or vanadium tubes for the low-temperature studies and 0.01-in. wall quartz tubes for some room-temperature runs.

III. ANALYSIS OF THE DATA

For convenience, before presentation of the data, the pertinent intensity relationships and details of interpretation will be summarized.

The magnetic structure factor is given by[17]:

$$\mathbf{F}=\sum_j p_j\mathbf{q}_j \exp 2\pi i(hx_j+ky_j+lz_j), \quad (1)$$

where p_j is the atomic scattering amplitude, proportional to the magnetic moment μ_j. $\mathbf{q}$ is a function of the unit vectors $\mathbf{e}$ and $\mathbf{K}$, parallel, respectively, to the scattering vector and magnetic moment.

$$\mathbf{q}=\mathbf{e}(\mathbf{e}\cdot\mathbf{K})-\mathbf{K}. \quad (2)$$

The intensity is proportional to the square of $\mathbf{F}$ averaged over the equivalent reflections and for a single spin axis structure can be written as

$$F_{\text{mag}}^2=\langle\mathbf{F}^*\cdot\mathbf{F}\rangle=\langle q^2\rangle[\textstyle\sum_j p_j \exp 2\pi i(hx_j+ky_j+lz_j)]^2. \quad (3)$$

$\langle q^2\rangle$ is the average, over the equivalent reflections, of $\sin^2\alpha$, where α is the angle between the spin axis and the scattering vector. For convenience, p has now been assigned a sign determined by $\mathbf{q}$ and is positive for moments parallel to the spin axis and negative for those antiparallel to it.

In the NiAs structure, the metal atoms are located at (0,0,0) and (0,0,1/2). Equation (3) reduces to

$$F_{\text{mag}}^2=\langle q^2\rangle(p^A\pm p^B)^2. \quad (4)$$

[15] D. E. Cox, W. J. Takei, R. C. Miller, and G. Shirane, J. Phys. Chem. Solids **23**, 863 (1962).
[16] P. Weiss and R. Forrer, Compt. Rend. **178**, 1670 (1924).
[17] O. Halpern and M. H. Johnson, Phys. Rev. **55**, 898 (1939).

p^A and p^B refer to the atoms at z equal to 0 and $\frac{1}{2}$, respectively. The positive sign is used for reflections with l even and the negative for l odd. Therefore, a ferromagnetic structure with the p's equal and positive gives a magnetic contribution only to the reflections with l even. Conversely, an antiferromagnetic structure has magnetic intensity only for reflections with l odd since the p's differ in sign. The value of $\langle q^2\rangle$ is[18]:

$$\langle q^2\rangle = 1-\frac{2}{3a^2}(h^2+k^2+hk)d^2\sin^2\Phi-\frac{l^2d^2}{c^2}\cos^2\Phi, \quad (5)$$

where Φ is the angle between the spin axis and c.

In some structures, a ferromagnetic or antiferromagnetic arrangement was derived which had a spin axis tilted from c. The intensity is given by

$$F^2=(1-A\sin^2\Phi-B\cos^2\Phi)(p^A\pm{}^Bp). \quad (6)$$

$\langle q^2\rangle$ has been simplified for convenience. For the cases with Φ between 0° and 90°, the possibility of another type of structure was considered. This was to assume that the sample consisted of two coexisting structures. One would have its spin axis parallel to c ($\langle q^2\rangle$ equal to $1-B$) and the other a spin axis perpendicular to c ($\langle q^2\rangle$ equal to $1-A$). If the mole fraction, $X_\perp$, of the perpendicularly oriented portion was $\sin^2\Phi$ and $X_\parallel$, $\cos^2\Phi$, the intensity of this mixture would be proportional to

$$\begin{aligned}F^2&=X_\perp\langle q^2\rangle_\perp(\mu^A\pm\mu^B)+X_\parallel\langle q^2\rangle_\parallel(p^A\pm p^B)\\&=[(1-A)\sin^2\Phi+(1-B)\cos^2\Phi](p^A\pm p^B)\\&=[1-A\sin^2\Phi-B\cos^2\Phi](p^A\pm p^B).\end{aligned}$$

This equation is identical to Eq. (6) for the tilted axis model. Thus, the two models cannot be differentiated and the magnitude of the atomic moments derived from the data would be the same. For convenience, the data will be discussed using the tilted axis model but it must be remembered that there is no *a priori* reason for eliminating the other model.

Equation (4) was derived for a single spin axis structure. However, there is another type of structure to which it can also be applied directly. Consider a magnetic structure in which the spins can be resolved into ferromagnetic components of magnitude μ_0 and antiferromagnetic components μ_1 along two independent axes. This is not the same as the mixture case considered in the preceding paragraph, since there is now only one structure present in the sample. Because of the atomic positions, the structure factors are such that the two components will diffract independently of each other.

$$\begin{aligned}F_{\text{mag}}{}^2&=\langle q_F{}^2\rangle(p_0{}^A+p_0{}^B)^2, \quad l=2n\\F_{\text{mag}}{}^2&=\langle q_{AF}{}^2\rangle(p_1{}^A-p_1{}^B)^2, \quad l=2n+1.\end{aligned} \quad (7)$$

By application of these equations to the data, the moment and Φ of the two components can be derived.

[18] G. Shirane, Acta Cryst. **12**, 282 (1959).

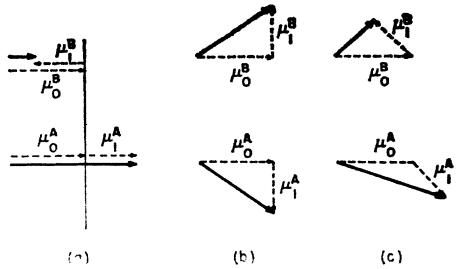

FIG. 5. Structures obtained by combining ferromagnetic and antiferromagnetic components. The angles between the spin axes of the two components are assumed to be: (a) 0°, (b) 90°, (c) between 0° and 90°.

However, an ambiguity arises in combining these components to obtain the actual structure. The angles, Φ, between the spin axes and c are known but not their rotational position about c. Consider the situation when the ferromagnetic and antiferromagnetic components have their spin axes perpendicular to c. Both the axes lie within (001) planes but their relative position within the plane is not known. There are three cases to be considered. The angle between the spin axes of the components could be: (1), 0°; (2), 90°; and (3) between 0° and 90°. For (1), since the spin axes of the components are parallel to each other, they combine as illustrated in Fig. 5(a). The resultant structure has parallel but unequal moments alternating along c. If the antiferromagnetic component had been the larger one, the structure would have been ferrimagnetic. For case (2), the axes are within the (001) plane but perpendicular to each other with a resultant structure as shown in Fig. 5(b). The spins are now equal in magnitude but alternate by an angle $\Theta/2$ with respect to the ferromagnetic component axis. This is a canted spin structure. For case (3) with an intermediate angle between the component axes, the resultant structure, shown in Fig. 5(c), has canted unequal moments. These three cases cannot be differentiated by the present diffraction data. However, there is no evidence for the presence of unequal moments in this system and the assumption of parallel spin axes results in unreasonable moment magnitudes in some cases. Therefore, it was concluded that case (2), the canted spin structure with equal spins, was the most probable one and the results will be presented in terms of this structure.

IV. MAGNETIC AND NEUTRON DIFFRACTION RESULTS

A. CrSb

The results of the magnetic measurements of CrSb, shown in Table II, agree with previous reports.[6,7] The structure obtained by room-temperature neutron diffraction experiments is in agreement with that of Snow.[4] Ferromagnetic (001) layers are coupled antiferromagnetically with the spin axis parallel to c. If, following Snow, the Mn^{+2} form factor is used, a moment of 2.6 μ_B

TABLE II. Magnetic properties of $Mn_{1-x}Cr_xSb$. T_C and T_N are the Curie and Néel temperatures; θ_p, the asymptotic Curie temperature from the susceptibility measurements; $2S$, twice the number of unpaired spins in the paramagnetic region as derived from the Curie constant; $\mu_{\infty,0}$, the measured atomic saturation moment extrapolated to infinite field and 0°K.

X	T_C (°K)	T_N (°K)	θ_p (°K)	$2S$	$\mu_{\infty,0}$ (μ_B)
0 (annealed)	600	···	600	3.4_3	3.5_3
0 (quenched)	565	···	525	3.9_0	3.3_7
0.25	505	···	505	3.2_3	2.8_7
0.51	390	···	410	2.9_3	1.8_5
0.7	255	500	260	3.1_5	0.9
0.75	175	550	185	3.3_0	0.7
0.8	130	590	175	3.2_0	0.4
0.85	(<77)	620	45	3.2_2	
1.0	···	705	−625	3.8_9	

is calculated compared to his 2.7 μ_B. However, the use of the Cr^{+3} form factor as obtained from Cr_2O_3[19] made it evident that the proper moment was 2.84 μ_B at room temperature which extrapolates to 3.0 μ_B at 0°K by the Brillouin function. Figure 6 shows the form factors calculated using this moment as well as those from Cr_2O_3. The Mn^{+2} form factor curve is also shown for comparison. A composite form factor curve was drawn from the two sets of points and used in the subsequent calculations for the solid solutions. It may be noted that 3 μ_B is smaller than the 3.8$_9$ μ_B expected on the basis of the susceptibility measurements. A possible reason for this discrepancy may be that the susceptibility measurements could not be extended sufficiently into the paramagnetic region to permit determination of the proper slope. It is also possible that there is a component of the Cr moment which does not order at 300°K.

B. MnSb

The magnetic structure derived from the neutron diffraction data for both the annealed and quenched MnSb at 77°K was basically that of a ferromagnetic structure with the spin axis perpendicular to c. The data for the quenched MnSb are given in Table III and compared with the calculated intensities assuming spin axes perpendicular and parallel to c. In addition to the expected ferromagnetic reflections, there are very small peaks which cannot be indexed on the basis of the chemical unit cell or small multiples of it. Accurate positional and intensity measurements could not be made but they seem to occur in pairs associated with the (001) and (101) positions as would be expected for a sinusoidally modulated antiferromagnetic structure. The magnetic component involved is extremely small, representing only a small perturbation of the basic ferromagnetic structure and does not materially affect the main conclusions to be drawn.

During the initial intensity calculations, the Mn^{+2} form factor was used. It was noted that this resulted in an atomic ferromagnetic moment larger than that obtained from the magnetic saturation measurements. Therefore, new form-factor values were computed using the intensity data from the ferromagnetic reflections and the atomic moments obtained from the magnetization measurements. They are shown in Fig. 7. It can be seen that the points are above the Mn^{+2} curve. Also shown is the form factor for Mn obtained by Roberts[20] from MnBi. A smooth curve was drawn through the points and used for the subsequent calculations. It should be noted that this is a small change and does not affect the conclusions as to the spin directions.

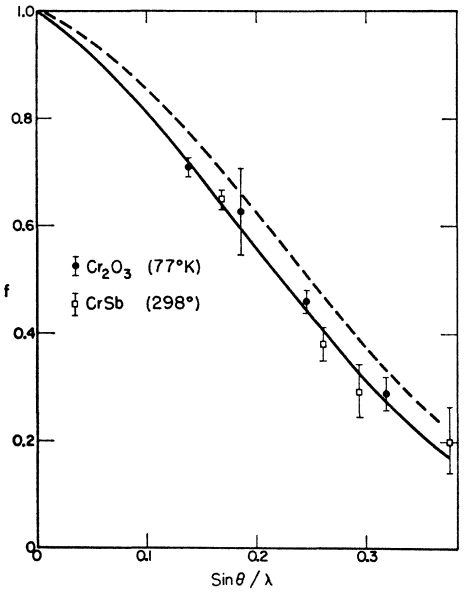

FIG. 6. Observed form factors for Cr. Moments are assumed to be 2.99 μ_B for Cr_2O_3 (reference 15) and 2.84 μ_B for CrSb.

At room temperature, the results from the two MnSb samples differed from each other. They also differed from those reported by Pickart and Nathans,[5] who reported a spin axis parallel to c. The annealed MnSb, whose diffraction pattern is shown in Fig. 8, was found

TABLE III. Neutron diffraction intensities for quenched MnSb. Calculated intensities include a temperature factor B of 0.4×10^{-16} Å^2 at 77°K and 0.8×10^{-16} Å^2 at 300°K. Magnetic contributions calculated utilizing the measured saturation moments of 3.35 μ_B at 77°K and 2.90 μ_B at 300°K. Φ is the angle between the spin axis and c.

		77°K			300°K			
	I_{nuc} calc	I_{tot} ($\Phi=0$)	I_{tot} ($\Phi=90$)	I_{obs}	I_{calc} ($\Phi=0$)	I_{calc} ($\Phi=90$)	I_{calc} ($\Phi=60$)	I_{obs}
(100)	188	436	311	329	368	276	299	306
(101)	152	150	150	146	146	146	146	149
(002)	83	82	126	114	79	111	103	87
(102)	4	46	100	102	34	66	58	70
(110)	5	48	27	22	36	20	24	21
(200)	50	73	58	57				
(201)	49							
(103)	49	283	283	262				
(112)	180							
(202)	2	21	18	15				

[19] D. E. Cox, W. J. Takei, and G. Shirane (to be published).

[20] B. W. Roberts, Phys. Rev. **104**, 607 (1956).

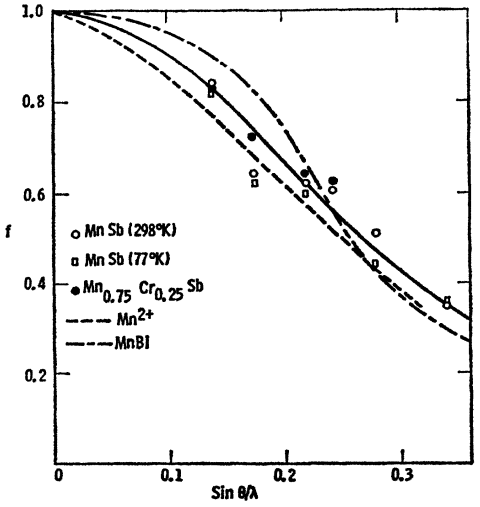

FIG. 7. Observed form factors for Mn. Moments used: 3.53 μ_B for MnSb at 77°K, 3.26 μ_B for MnSb at 300°K, and 2.51 μ_B for $Mn_{0.75}Cr_{0.25}Sb$. MnBi values from Roberts (reference 20).

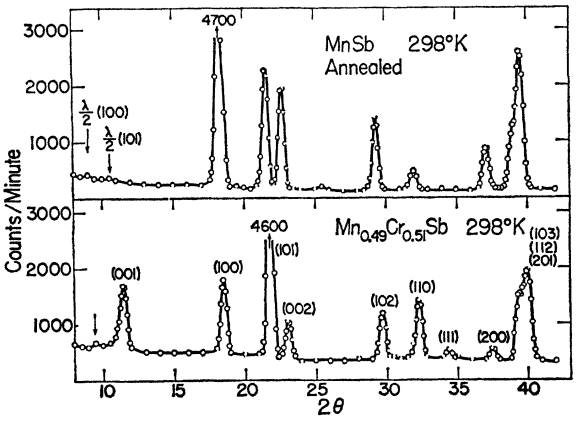

FIG. 8. Neutron diffraction pattern for annealed MnSb and $Mn_{0.49}Cr_{0.51}Sb$ at 300°K. Thin-walled, 3/8-in.-diam, cylindrical quartz sample holder. Wavelength, 1.14 Å.

to have a ferromagnetic structure with a spin axis perpendicular to c. One crucial point leading to this conclusion was that there was a significant magnetic contribution to the (002) reflection. This would not be allowed by a spin axis parallel to c since $\langle q^2 \rangle$ would then be zero. Also, the magnitude of (102), which has a very small nuclear component, was much too large. This structure was tested by making measurements of the ratio between the nuclear and total intensity of various reflections. The nuclear intensities were measured by eliminating the magnetic contributions using two different methods. One was by scanning a sample heated to a temperature (625°K) above the Curie point. The second method was to scan a sample in a magnetic field applied parallel to the scattering vector. The results obtained are shown in Table IV with the calculated values for spins parallel and perpendicular to c. The best agreement is obtained by assuming a spin axis perpendicular to c although application of a magnetic field did not reduce the intensity of (102) sufficiently. The high-temperature experiment did give the proper ratio for this peak. This could be explained if the perpendicular to the (102) plane was along or close to a "hard" direction of magnetization. If the anisotropy was large, the spins would not be oriented by the field in the desired direction for this reflection and thus the magnetic contribution would not be completely eliminated.

TABLE IV. Ratio, R, between nuclear and total intensities. Magnetic contribution eliminated for R_{mag} by application of a magnetic field and for R_{heat} by heating above the Curie temperature. Φ is the angle between the spin axis and c.

Refl.	R_{mag}	R_{heat}	R_{calc} ($\Phi=90°$)	R_{calc} ($\Phi=0°$)
(100)	0.63	0.59	0.61	0.44
(101)	0.98	0.99	1.00	1.00
(002)	0.72	0.56	0.66	1.00
(102)	0.22	0.03	0.03	0.07

The room temperature neutron diffraction data for quenched MnSb are given in Table III. The observed intensities are not in agreement with either a parallel or perpendicular spin orientation. The best fit seems to be obtained with an intermediate orientation, Φ equal to 60°.

The neutron diffraction data for the two MnSb samples and the results reported by Pickart andNathans could be explained by a spin flip occurring at a variable temperature. Further evidence for this "spin flip" was given by a study of the temperature variation of the magnetization. The results are shown in Fig. 9. The high-field curves for the annealed sample follow a normal Brillouin curve with an extrapolated moment

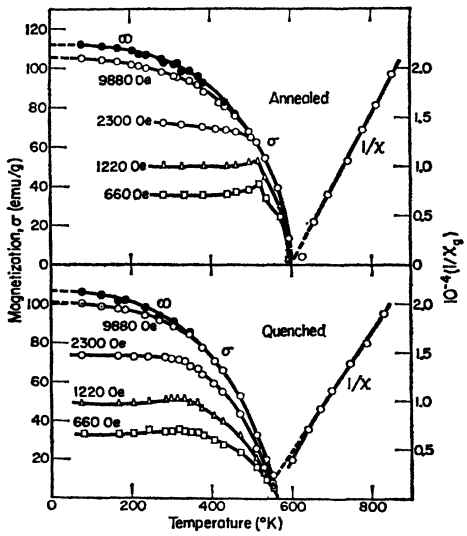

FIG. 9. Magnetization and inverse susceptibility as a function of temperature for quenched and annealed MnSb. Values for quenched MnSb are those obtained on heating. On cooling, the curves approach those of the annealed sample.

of 3.5 μ_B at 0°K and infinite field. This is in agreement with the results of Hirone *et al.*[6] and of Guillaud,[21] who reported 3.49 and 3.53 μ_B, respectively. However, the low-field curves show a pronounced peak at approximately 520°K. This behavior is similar to that reported by Guillaud[21] for Mn_2Sb which shows a "spin flip" at approximately 240°K. The properties of quenched MnSb are significantly different. The standard magnetic parameters are given in Table II. The extrapolated moment, 3.3$_7$ μ_B, is smaller than that of the annealed sample, as is the Curie temperature. Of particular interest is the fact that the peaks in the low-field saturation curves are now broad ones centered at approximately 320°K. This is in agreement with the neutron diffraction results which found an intermediate structure at 300°K. These magnetic properties are not the same after heating to 850°K, however, as then the susceptibility and magnetization curves on cooling follow those of the annealed sample. The extrapolated moment and Curie temperature are higher and the spin flip is at approximately 510°K.

This dependence of the magnetic properties could be explained as a consequence of a composition dependence of the flipping temperature. The equilibrium composition of MnSb is deficient in Sb above 870°K according to Hanson.[22] Thus, rapid cooling would result in a MnSb phase deficient in Sb plus free Sb (or Sb-rich component). Guillaud[21] has reported the magnetic properties of MnSb deficient in Sb. The Curie temperature and magnetic moment are lower than in the stoichiometric compound. On the basis of his values, it is estimated that the quenched sample would have a 1% deficiency. The corresponding amount of free Sb would not be detected by the x-ray study. Heating the sample to 850°K followed by slow cooling would allow the Sb to diffuse into the compound and approach the stoichiometric composition. This would account for the different magnetic properties on heating and cooling.

The sample studied by Pickart and Nathans[5] was reported to have an extrapolated atomic moment of 3.3 μ_B. This low moment could be correlated with a larger Sb deficiency and, thus, a lower flipping temperature. Their data would then be explained as resulting from their sample at room temperature being above this transition point and, therefore, having a spin axis parallel to *c*.

The "best" sample to be studied had a "spin flip" temperature, 520°K, close to the Curie temperature of 600°K. If it assumed that this sample was also slightly off-stoichiometry, then the true transition temperature might be higher. It may be possible that the spin structure with the axis parallel to *c* is not a stable phase in stoichiometric MnSb.

It may be noted that this spin flip for MnSb is of the same type as that found for the isostructural compound MnBi reported by Roberts.[20] At room temperature, MnBi has a ferromagnetic structure with the spin axis parallel to *c*. At 77°K, a structure intermediate between a parallel and perpendicular spin orientation was found. Differences were noted in the range of this transition for two samples prepared under different conditions.

[21] C. Guillaud, Ann. Phys. (Paris) 4, 671 (1949).
[22] M. Hanson, *Constitution of Binary Alloys* (McGraw-Hill Book Company, Inc., New York, 1958), 2nd ed.

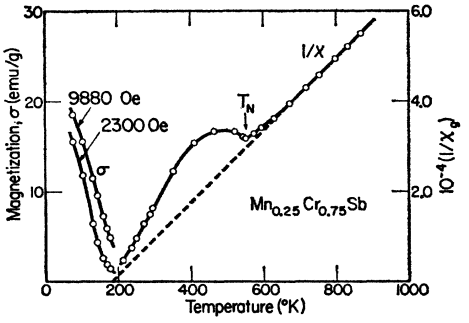

FIG. 10. Magnetization and inverse susceptibility as a function of temperature for $Mn_{0.25}Cr_{0.75}Sb$.

C. $Mn_{1-x}Cr_xSb$

The shape of the magnetization and susceptibility curves for the solid solutions are the same as those previously reported.[6,7] For this reason, the curves will not be presented except, as an example, those for $Mn_{0.75}Cr_{0.25}Sb$ in Fig. 10. All samples with x equal to or greater than 0.7 showed the peak in the inverse susceptibility curve and the Néel temperature was taken at the minimum as indicated. The measured magnetic parameters are given in Table II. They are in agreement with the previous values taking into consideration the difficulty of making the extrapolations in some cases.

The compounds and the temperatures at which neutron diffraction studies of the solid solutions were made can be determined by the location of the entries in Table V. Most scans were conducted to a 2θ value of 70°, corresponding to a value of 0.5 for $\sin\theta/\lambda$, so that many reflections were available which did not have a significant magnetic contribution. No indication was obtained of any chemical ordering of the metals in the solid solutions. This lack of ordering would seem to make the presence of independent Cr and Mn spin systems as proposed by Lotgering and Gorter[7] unlikely.

TABLE V. Moment in μ_B of antiferromagnetic component perpendicular to *c* in $Mn_{1-x}Cr_xSb$. *S* refers to presence of satellites.

X	300°K	77°K	4.2°K
0 (annealed)	0	*S*	
0 (quenched)	0	*S*	
0.25	0.5		
0.51	1.8		
0.70	2.1_5	2.4_0	
0.75	1.2_8	2.8_1	
0.80	0.3	0.8	1.0
0.85		~0.2	~0.2
1.0	0		

The additional peaks requiring an increase of the unit cell size, as predicted by the model of Hirone and Adachi,[8] are not present. The canted spin model predicts, in the ferromagnetic region, the occurrence of antiferromagnetic reflections. This prediction is in agreement with the experimental data as is shown by the development of (001) reflections. Figure 11 shows the room temperature intensity of this reflection which must be entirely magnetic except for an extremely small half-wavelength component which has been subtracted. A magnetic (001) reflection can arise only from an antiferromagnetic component perpendicular to c. A CrSb-type structure with a spin axis along c would have no contribution to (001) since the "q" value would be zero. The magnitude of this perpendicular component is given in Table V.

In addition to the contribution from the perpendicular antiferromagnetic component, the diffraction data show the magnetic intensity which would be expected on the basis of the magnetic measurements. Thus, in the ferromagnetic region, each peak with l even had a magnetic component corresponding to a ferromagnetic spin arrangement with an axis perpendicular to c. The magnetic intensity of two such peaks at room temperature is shown in Fig. 11. As would be expected from the variation of the saturation moment, the intensity decreases with increasing Cr content. In the antiferromagnetic region, the reflections with l odd had a magnetic contribution corresponding to a CrSb-type structure with the spin axis parallel to c. The variation of magnetic intensity for (101) is shown in Fig. 11. It has been corrected for the simultaneous contribution due to the antiferromagnetic component perpendicular to c.

The resultant magnetic structure is obtained by combining the various components as indicated in Sec. III. In the ferromagnetic region, the two components combine to form a canted spin structure. As an example, the room-temperature data for $Mn_{0.49}Cr_{0.51}Sb$ are shown in Fig. 8 and Table VI. At this composition, only Sb contributes to the nuclear intensity since the Mn and Cr scattering lengths of -0.36 and $+0.35\times10^{-12}$ cm, respectively, average to zero. The magnetic intensity was calculated using $1.36\,\mu_B$ for the ferromagnetic component as determined by the magnetization measurements and $1.80\,\mu_B$ for the antiferromagnetic component. Both components lie in the basal plane. Combining these two components on the assumption that their spin axes are perpendicular gives a canted spin structure composed of moments of $2.26\,\mu_B$ with a cant angle of 103°. Application of the observed $\sigma_{300°K}/\sigma_{0°K}$ ratio of 0.73 gives an extrapolated moment of $3.1\,\mu_B$ at 0°K. This extrapolation assumes that both components follow the same Brillouin curve in this case. This would seem to be a reasonable approximation on the basis of the study of $Mn_{0.25}Cr_{0.75}$ which will be presented later. If the ferromagnetic and antiferromagnetic components had been assumed to have parallel spin axes, the resultant would have been ferrimagnetic, composed of an unreasonably large moment of $4.3\,\mu_B$ alternating with one of $-0.6\,\mu_B$ at 0°K.

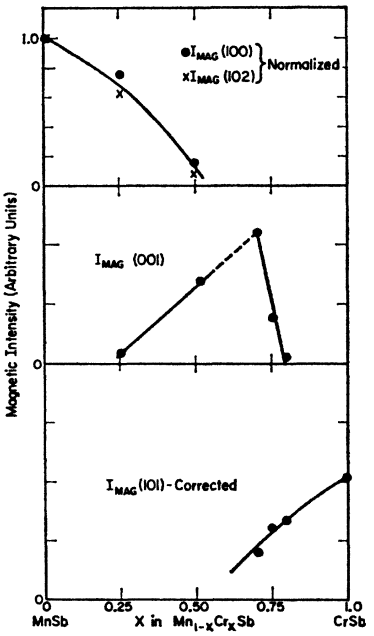

FIG. 11. Magnetic intensity of $Mn_{1-x}Cr_xSb$ solid solutions. Intensities of (100) and (102) are normalized to equal one for MnSb. Intensity of (101) has been corrected for the contribution due to antiferromagnetic component perpendicular to c as discussed in text.

TABLE VI. Neutron diffraction intensities of $Mn_{0.49}Cr_{0.51}Sb$ at room temperature. Temperature factor of 0.6×10^{-16} Å^2 included. Ferromagnetic moment of $1.36\,\mu_B$ and antiferromagnetic moment of $1.80\,\mu_B$ used.

		Calculated			
Ref.	I_{nuc}	I_{mag} ferro	I_{mag} antiferro	I_{total}	Observed I_0
(001)			68	68	73
(100)	34	18		52	70
(101)	159		57	216	209
(002)	29	6		35	34
(102)	26	12		38	45
(110)	44	2		46	60
(113)			8	11	13
(003)			3		
(200)	8	2		10	13
(201)	43		4	159	167
(103)	43		8		
(112)	58	3			
(202)	10	2		12	12
(004)	7			7	6
(210)	9	1		100	102
(104)	9				
(211)	52		2		
(203)	26		1		
(212)	17			67	67
(300)	17				
(114)	33				
(204)	6			83	80
(213)	35				
(302)	24				
(105)	18				
(320)	10			10	13

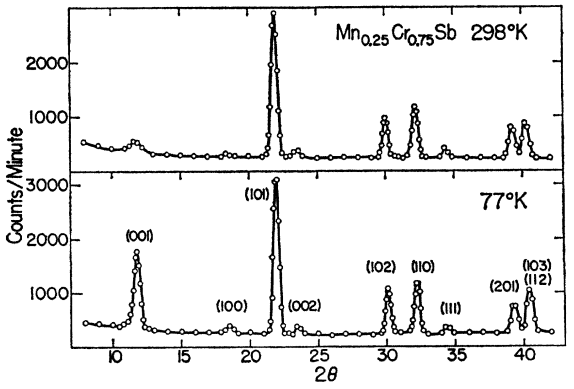

FIG. 12. Neutron diffraction patterns of $Mn_{0.25}Cr_{0.75}Sb$ at 77°K and 300°K. Thin-walled, 3/8-in. diameter, cylindrical vanadium sample holder used with wavelength of 1.14 Å.

Figure 11 shows that the (001) reflection also occurs in the antiferromagnetic region. However, the significance of this peak is fundamentally different from that previously. In the ferromagnetic region, it showed that an entirely different type of structure was present, namely, a canted spin arrangement. In this case, however, it simply confirms that the structure is antiferromagnetic but with a tilted spin axis. It is a transition structure between the CrSb type, with the spin axis parallel to c, and the canted spin structure with the spins perpendicular to c.

An illustration of a compound which can show ferromagnetic and antiferromagnetic transitions is $Mn_{0.25}Cr_{0.75}Sb$. This compound has a Curie temperature of 175°K and a Néel temperature of 550°K. The data taken at 77 and 300°K are shown in Fig. 12 and Table VII. At 77°K, the magnetic structure is made up of a small ferromagnetic component of 0.65 μ_B and a large antiferromagnetic one of 2.81 μ_B. The resultant is a moment of 2.88 μ_B with a cant angle of 154°. In the antiferromagnetic region at 300°K, a small (001) reflection still remains. This is accounted for by a tilt in the spin axis of approximately 30° away from c to give the calculated intensities in Table VII.

TABLE VII. Neutron diffraction intensities of $Mn_{0.25}Cr_{0.75}Sb$. For 300°K, a temperature factor B of 0.5×10^{-16} Å^2, is included.

	77°K					300°K		
	I_{nuc} (calc)	I_F 0.65 μ_B	I_{AF} 2.81 μ_B	I_{tot} (calc)	I_0	I_{AF} 2.65 μ_B $\Phi=30°$	I_{tot} (calc)	I_0
(001)			158	158	157	31	30	28
(100)	4	4		8	14	4	4	6
(101)	149		110	259	261	94	238	245
(002)	13	1		14	14		13	13
(102)	73	2		75	72		73	65
(110)	82	2		84	94		78	84
(111)			18	18	15	22	20	12
(003)			4	4	6	1	1	<3
(201)	49		9	58	58	11	54	58
(112)	29	1						
(103)	47		13	100	88	4	71	71
(202)	35	1		36	43		32	31
(004)	14	1		15	15		12	12
(211)	61		2			6		
(203)	2		2	98	94	2	90	84
(104)	31							
(122)	48			78	78		42	43
(300)	30						26	27
(114)	58			58	49		49	40

Another interesting phenomenon which was studied was the temperature variation of the (001) peak between 300 and 77°K for the 75% Cr compound. It was found to show a considerable thermal hysteresis. On cooling, the intensity of the (001) reflection increased rapidly below 220°K so that at the Curie temperature of 175° it was close to its 77°K value. However, on heating, the (001) intensity decreased only gradually and did not approach its original value until room temperature was reached. The magnetization measurements on this sample showed no hysteresis of the ferromagnetic ordering. These results can be interpreted as a consequence of the following structural changes. As the sample is cooled, the angle between the antiferromagnetic axis and c starts to increase rapidly at approximately 50° above the Curie temperature. At the Curie temperature the spin axis is perpendicular to c and at this point, a ferromagnetic component starts to order resulting in a canted structure. On heating, after the ferromagnetic component disappears, the antiferromagnetic axis approaches the c axis only gradually. A similar explanation could be given in terms of the model using the mixture of two structures.

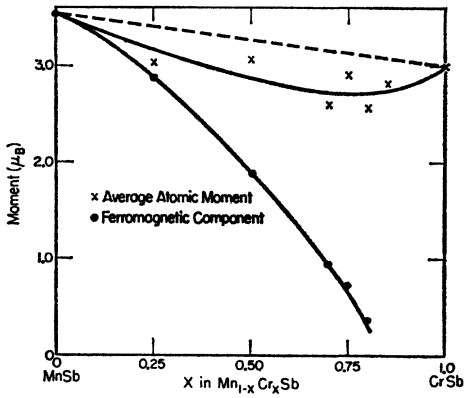

FIG. 13. Moments of $Mn_{1-x}Cr_xSb$ solid solutions at 0°K. The average atomic moment is obtained by combining the ferromagnetic component as determined by the magnetization measurements with the antiferromagnetic component from the neutron diffraction results.

It was remarked previously that, in the ferromagnetic region with increasing Cr content, there is a rapid decrease in the observed atomic moment as determined by magnetization measurements. It can now be seen that this decrease is due to the canting of the spins. Figure 13 shows the total moment obtained for each composition. The values quoted are those appropriate to 0°K, extrapolated by means of a Brillouin function. The dashed line indicates the moments calculated for a composition average assuming 3.53 and 3.0 μ_B for Mn and Cr, respectively. As can be seen, the observed values are close to this line, lying slightly below it. This

small "loss of moment" is similar to that found in othe-solid solution systems such as Fe_2O_3-$FeTiO_3$,[23] Fe_2O_3r V_2O_3,[15] and $MnFe_2O_4$-$MnCr_2O_4$.[24]

V. DISCUSSION

The results for MnSb-CrSb solid solutions are summarized by the magnetic phase diagram shown in Fig. 14 and the structures illustrated in Fig. 15. This diagram has been simplified and is qualitatively similar to that of de Gennes, Fig. 2(b). On the left, the stable structure at high temperature is of the MnSb type shown in Fig. 15(a) with a ferromagnetic arrangement of spins perpendicular to c. A phase line is indicated by line (A), below which the structure is a canted one as in Fig. 15(b). The exact location of this phase line has not been determined by this study. The corresponding phase line between an antiferromagnetic and a canted spin structure is that determined by the magnetization measurements. The region between this line and the dash-dot

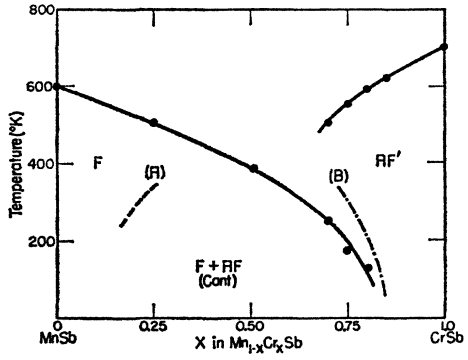

FIG. 14. Proposed magnetic phase diagram for $Mn_{1-x}Cr_xSb$ solid solutions. F and AF refer to ferromagnetic and antiferromagnetic structures, respectively. Lines (A) and (B) explained in text.

line (B) indicates the region in which the transition is occurring from the CrSb-type structure, with the spin axis along c as in Fig. 15(d), to the canted structure, with the spin axis lying in the (001) plane. In this antiferromagnetic region, the spins are either tilted away from c as in Fig. 15(c) or there are two coexisting structures as discussed previously.

There are several other structures which, although not indicated in Fig. 14, may also be present in this system. One is the structure found for $Mn_{0.2}Cr_{0.8}Sb$ at 4.2°K by Pickart and Nathans.[5] Attempts to locate this phase in the 80 and 85% Cr samples were not successful. It is possible that preparative variations could affect the stability range of this phase and that if the 75% Cr sample or an intermediate composition had been examined at 4.2°K, it might have been found.

Another possible phase is the ferromagnetic structure

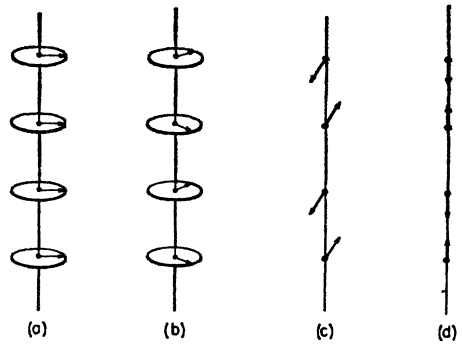

FIG. 15. Magnetic structures present in $Mn_{1-x}Cr_xSb$ solid solutions.

found in MnSb with the spin parallel to c. If this structure is truly characteristic of stoichiometric MnSb, then it should extend into the solid solution region. However, since the flipping temperature is so close to the Curie temperature in the present sample of MnSb, it might be expected to have only a small region of stability.

The third possible structure in the system is that giving rise to the "satellites" found in MnSb at 77°K. Since they seem to be associated with the reflections with l odd, they may correspond to a sinusoidal modulation of an antiferromagnetic component. Clarification of this structure, however, must await the study of single crystals in order to increase the accuracy of the data.

Several mechanisms have been proposed to account for the origin of canted spin structures. Dzialoshinski[25] and Moriya[26] have derived these structures as a consequence of an anisotropic superexchange interaction due to spin-orbit coupling. However, it is a small effect, being of the order of $\Delta g/g$ where g is the gyromagnetic ratio and Δg its deviation from the free electron value. Its application, in general, has been limited to the explanation of the occurrence of parasitic ferromagnetism in basically antiferromagnetic compounds such as αFe_2O_3. Structures similar to the canted spin arrangements are the triangular spin configurations as derived by Yafet and Kittel,[27] Kaplan,[28] and Hirone and Adachi.[8] These authors used the molecular field approximation and assumed a negative interaction between atoms in the feromagnetic sublattice of a ferrimagnetic or antiferromagnetic structure.

The theoretical analysis which has the best agreement with the present results is that of de Gennes. As discussed in the introduction, canted spin structures were derived by considering the effects of double exchange on an antiferromagnetic structure. Predictions were made which are in agreement with the experimental results. These are:

[23] G. Shirane, D. E. Cox, W. J. Takei, and S. L. Ruby, J. Phys. Soc. Japan **17**, 1598 (1962).
[24] S. J. Pickart and R. Nathans, Phys. Rev. **116**, 317 (1959).
[25] I. Dzialoshinski, J. Phys. Chem. Solids **4**, 241 (1958).
[26] T. Moriya, Phys. Rev. **120**, 91 (1960).
[27] Y. Yafet and C. Kittel, Phys. Rev. **87**, 290 (1952).
[28] T. A. Kaplan, Phys. Rev. **116**, 888 (1959).

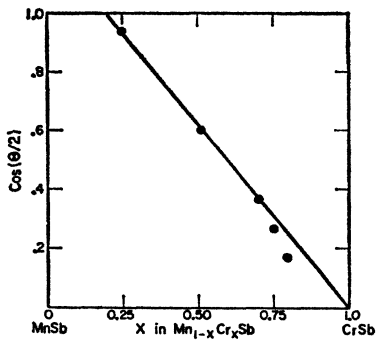

FIG. 16. Cosine of half of the cant angle, Θ, as a function of composition for $Mn_{1-x}Cr_xSb$ solid solutions at 0°K.

(1) Canted spin structures are found.

(2) The generalized magnetic phase diagram, Fig. 2(b), is of the same form as that found, Fig. 14.

(3) The inverse susceptibility curves have a peak as indicated by the typical example of $Mn_{0.25}Cr_{0.75}Sb$ in Fig. 10.

(4) A linear variation of $\cos(\Theta/2)$ as a function of carrier concentration and therefore of composition was predicted. The experimental results are shown in Fig. 16. The values plotted are those appropriate to 0°K as the study of the 75% Cr sample showed that, after an initial change, there was only a small variation of angle with temperature.

(5) In the magnetic phase diagram of de Gennes, Fig. 2(b), there is one composition which passes directly from a canted spin structure to paramagnetism on heating. For increasing carrier concentration, this is the composition at which the ordered phase at high temperature changes from an antiferromagnetic to a ferromagnetic structure. It was predicted that this composition would have a cant angle of 103°. From Fig. 14, it is estimated that this composition is approximately $Mn_{0.4}Cr_{0.6}Sb$. From Fig. 16, this would have a cant angle of about 113°, in agreement with the prediction.

It is perhaps somewhat surprising that a linear variation of $\cos(\theta/2)$ is obtained over such a wide composition range in view of the fact that double exchange theories have generally been confined to a rather narrow range. Moreover, owing to the lack of conductivity data direct evidence concerning the mobility of the carriers in this system is not available. The possibility that a suitable molecular field approach, for example, could give equally good agreement with the experimental findings should therefore not be overlooked. However, if double exchange is assumed to occur throughout the system, it may be concluded that the experimental results provide strong support for the theory of de Gennes.

There are several points of interest which could be studied further by neutron diffraction. These include: (a) direct observation of the spin flip in MnSb; (b) the sinusoidally modulated structure in MnSb at 77°K; (c) the exact location of the phase line (A) in the magnetic phase diagram, Fig. 14; (d) the possibility of structures such as in Figs. 5(a) and 5(c); these structures, though improbable, could be tested by neutron diffraction data taken with an applied magnetic field; (e) the phase found by Pickart and Nathans for $Mn_{0.8}Cr_{0.2}Sb$. Unfortunately, before these points could be investigated, the reactor operations were terminated. However, the main features of the MnSb-CrSb systems are now well established and clarification of these other features will be undertaken at a later date.

ACKNOWLEDGMENTS

The authors wish to thank Dr. R. Nathans of the Brookhaven National Laboratory, Dr. S. J. Pickart of the Naval Ordnance Laboratory, and Dr. R. R. Heikes and Dr. A. J. Cornish of these Laboratories for helpful discussions. The preparation of one of the MnSb samples by Dr. Cornish has been mentioned previously. The assistance of M. Janocko with some of the preparative and x-ray experiments is also gratefully acknowledged.